Martin Picard, Darmyn Ritchie, Kathryn J. Wright, Caroline Romestaing, Melissa M. Thomas, Sharon L. Rowan, Tanja Taivassalo, and Russell T. Hepple

Mitochondrial functional impairment with aging is exaggerated in isolated mitochondria compared to permeabilized myofibers

Published in:
Aging Cell (2010) 9, pp1032-1046.

doi: 10.1111/j.1474-9726.2010.00628.x
http://onlinelibrary.wiley.com/doi/10.1111/j.1474-9726.2010.00628.x/full

Aging Cell (2010) **9,** pp1032–1046 Doi: 10.1111/j.1474-9726.2010.00628.x

Mitochondrial functional impairment with aging is exaggerated in isolated mitochondria compared to permeabilized myofibers

Martin Picard,[1,*] Darmyn Ritchie,[2,*] Kathryn J. Wright,[2] Caroline Romestaing,[3] Melissa M. Thomas,[2] Sharon L. Rowan,[2] Tanja Taivassalo[1] and Russell T. Hepple[2]

[1]Department of Kinesiology, McGill University, Montreal, QC H2W 1S4, Canada
[2]Muscle & Aging Laboratory, Faculty of Kinesiology and Faculty of Medicine, University of Calgary, Calgary, AB T2N 1N4, Canada
[3]Laboratoire de Physiologie Intégrative, Cellulaire et Moléculaire, Université de Lyon, Lyon, France

Summary

Mitochondria regulate cellular bioenergetics and apoptosis and have been implicated in aging. However, it remains unclear whether age-related loss of muscle mass, known as sarcopenia, is associated with abnormal mitochondrial function. Two technically different approaches have mainly been used to measure mitochondrial function: isolated mitochondria and permeabilized myofiber bundles, but the reliability of these measures in the context of sarcopenia has not been systematically assessed before. A key difference between these approaches is that contrary to isolated mitochondria, permeabilized bundles contain the totality of fiber mitochondria where normal mitochondrial morphology and intracellular interactions are preserved. Using the gastrocnemius muscle from young adult and senescent rats, we show marked effects of aging on three primary indices of mitochondrial function (respiration, H_2O_2 emission, sensitivity of permeability transition pore to Ca^{2+}) when measured in isolated mitochondria, but to a much lesser degree when measured in permeabilized bundles. Our results clearly demonstrate that mitochondrial isolation procedures typically employed to study aged muscles expose functional impairments not seen *in situ*. We conclude that aging is associated with more modest changes in mitochondrial function in sarcopenic muscle than suggested previously from isolated organelle studies.

Correspondence
Russell T. Hepple, Faculty of Kinesiology, University of Calgary, 2500 University Dr NW, Calgary, AB T2N 1N4, Canada. Tel.: 403 220 8549; fax: 403 284 3553; e-mail: hepple@ucalgary.ca
*These authors contributed equally to this work.

Accepted for publication *29 August 2010*

Key words: isolated mitochondria; skinned fibers; aging; skeletal muscle; sarcopenia.

Introduction

Mitochondria play central roles in the regulation of cellular metabolism (Lesnefsky & Hoppel, 2006) and apoptosis (Manoli *et al.*, 2007; Wenz *et al.*, 2009). Likewise, several metabolic changes occur with muscle atrophy (Lecker *et al.*, 2004), and recent evidence suggests that mitochondrial function can be a key regulator of the atrophic process (Romanello *et al.*, 2010). For this and other reasons, age-related changes in mitochondrial function have been implicated in the decline of muscle mass and function with aging known as sarcopenia (Wanagat *et al.*, 2001; Terman & Brunk, 2004; Hiona & Leeuwenburgh, 2008). The isolation of mitochondria from skeletal muscle is a widely employed method in studies examining mitochondrial function under various conditions, including aging (Frezza *et al.*, 2007b; Lanza & Nair, 2009). Such studies have demonstrated significant alterations in a variety of indices of mitochondrial function in aged skeletal muscles including reduced maximal ATP-generating capacity (Drew *et al.*, 2003), reduced maximal respiratory capacity (Chabi *et al.*, 2008), increased reactive oxygen species (ROS) generation (Capel *et al.*, 2004; Mansouri *et al.*, 2006; Muller *et al.*, 2007), and impaired function of the mitochondrial permeability transition pore (mPTP) (Seo *et al.*, 2008). While these studies appear to reveal physiologically relevant alterations in mitochondrial function, the methods employed do not take into consideration the complex structural arrangement of mitochondria *in vivo* (Bakeeva *et al.*, 1978; Ogata & Yamasaki, 1997) nor the potential for the isolation process to expose vulnerabilities in aged mitochondria that are not evident *in vivo*. Mitochondria are dynamic organelles that exhibit varying degrees of a mitochondrial network in skeletal muscle (Kayar *et al.*, 1988; Ogata & Yamasaki, 1997; Shaw *et al.*, 2008), and this network facilitates functional interactions between mitochondria and other cytoskeletal elements (Benard *et al.*, 2007; Detmer & Chan, 2007; Romanello *et al.*, 2010; Saks *et al.*, 2010). This structural arrangement is lost during mitochondrial isolation procedures, and therefore, the assumption that mitochondria isolated from skeletal muscle should behave as they would *in vivo* is not a trivial concern.

In addition to disrupted structure upon isolation, most mitochondrial isolation methods yield 10–20% of the mitochondria within muscle (Kuznetsov *et al.*, 2008; Figueiredo *et al.*, 2009), which, because of isolation of specific sub-populations of mitochondria, may result in important bias (Piper *et al.*, 1985;

Kuznetsov *et al.*, 2008). Finally, it has been suggested that mitochondria from aged muscles become larger and more fragile than their younger counterparts (Terman & Brunk, 2004), and depending upon how this impacts survival during isolation adds to concerns about how accurate and/or complete the representation of mitochondria with aging are following isolation methods (Tonkonogi *et al.*, 2003; Figueiredo *et al.*, 2008).

A more recent and routinely employed approach to study mitochondrial function in skeletal muscle involves gentle dissection and chemical permeabilization of the sarcolemma to produce permeabilized myofiber bundles. Unlike isolated mitochondrial preparations, this method permits representation of all mitochondria within a muscle fiber and preserves mitochondrial structural interactions and morphology (Kuznetsov *et al.*, 2008). The only prior studies to use the permeabilized fiber approach in an aging context did not provide data concerning the degree of muscle atrophy (Tonkonogi *et al.*, 2003; Hutter *et al.*, 2007); no prior study has therefore applied this method to study mitochondrial function in a muscle where sarcopenia is well established.

Despite the concerns noted previously, to date, there has been no systematic comparison of mitochondrial function in aged muscles between isolated mitochondria and permeabilized myofiber bundles. To this end, we examined three primary indices of mitochondrial function in isolated mitochondria and saponin-permeabilized muscle fiber bundles from the mixed region of the gastrocnemius muscle in young adult (YA) and senescent (SEN) Fischer 344 × Brown Norway F1-hybrid (F344BN) rats: respiration, ROS emission, and mPTP sensitivity to Ca^{2+}. These measures of mitochondrial function were chosen because they are relevant to the decreased maximal ATP-generating capacity (Hepple *et al.*, 2004), increased oxidative damage accumulation (Mecocci *et al.*, 1999; Fugere *et al.*, 2006; Hepple *et al.*, 2008), and increased activation of apoptosis (Alway *et al.*, 2002; Dirks & Leeuwenburgh, 2002; Chabi *et al.*, 2008) previously observed in aging muscles. Furthermore, the SEN age represents a stage where sarcopenia is well established in the F344BN rat model (Brown & Hasser, 1996; Hagen *et al.*, 2004; Seo *et al.*, 2008), permitting relevant insight into the role of mitochondria in age-related muscle changes. Based upon the prevailing view that isolation procedures could selectively harvest the healthiest mitochondria (Tonkonogi *et al.*, 2003; Kuznetsov *et al.*, 2008), our *a priori* hypothesis was that isolated mitochondria would show less severe age-related impairments than permeabilized bundles.

Contrary to that hypothesis, we demonstrate that whereas isolated mitochondria from SEN muscle exhibit a marked reduction in respiratory capacity, higher H_2O_2 release under State III conditions, and increased mPTP sensitivity to Ca^{2+}, in SEN-permeabilized fiber bundles, respiratory capacity is reduced only under complex IV-driven respiration, there is no difference in H_2O_2 emission, and there is a lesser change in mPTP sensitivity to Ca^{2+}. In addition, our results indicate important qualitative differences in mitochondrial respiration and mPTP dynamics between YA- and SEN-isolated mitochondria, but not in permeabilized fiber bundles. As such, our findings indicate that routinely employed mitochondrial isolation procedures exaggerate functional age-related impairments in sarcopenic skeletal muscles. We conclude that the changes in mitochondrial function in a muscle where sarcopenia is well established are less severe than has typically been indicated by isolated organelle studies.

Results

Animal characteristics

The mass of the SEN animals (539 ± 30 g) was greater than that of the YA animals (400 ± 21 g; $P < 0.05$). On the other hand, gastrocnemius muscle mass was 38% less in SEN (1277 ± 36 mg) than YA (2054 ± 41 mg; $P < 0.05$), demonstrating an advanced state of sarcopenia.

Citrate synthase and complex IV activity in isolated mitochondria and fiber bundles

We measured mitochondrial protein yield in the mitochondrial isolation procedures, and citrate synthase (CS) and cytochrome c oxidase (COX) activities in both the isolated mitochondria and fiber bundles. Mitochondrial protein yield was very similar between age-groups (Fig. 1, inset). On the other hand, despite similar protein concentration of the isolated mitochondrial preparations in both age-groups, the CS (Fig. 1A) and COX (Fig. 1C) activities (normalized to 'mitochondrial' protein content) in isolated mitochondria were respectively 41% and 32% lower in the SEN age-group. These results from isolated mitochondria contrast with the very similar CS (Fig. 1B) and COX (Fig. 1D) activities between age-groups in the fiber bundle experiments. Note here that the data reported in Fig. 1B,D represent the activities measured in the fiber bundles used in H_2O_2 emission experiments and that similar results were obtained in the fiber bundles used in respirometry and Ca^{2+} retention capacity experiments (data not shown).

Characteristics of isolated mitochondria

For identical isolation procedures and matched protein concentration between age-groups, mitochondrial isolates from SEN muscle exhibited a markedly lower mitochondrial particle density, based on Mitotracker Red experiments (Fig. S1A,B). In fact, mitochondrial particle volume density (in μm^3 mitochondrial particles mm^{-3}) and fluorescence brightness density (in units of mean fluorescence intensity mm^{-3}) were 44% and 60% lower in the SEN sample, respectively (data not shown). This difference in volume density is similar in magnitude to the mean age differences in CS and COX activity (Fig. 1A,C), whereas the difference in fluorescence density parallels mean age differences in respiration (Fig. 3A) and H_2O_2 emission (Fig. 4A) per mg of protein in isolated mitochondria experiments. In addition to these results indicating lower mitochondrial content in isolates from SEN muscle, protein content of representative subunits of complexes

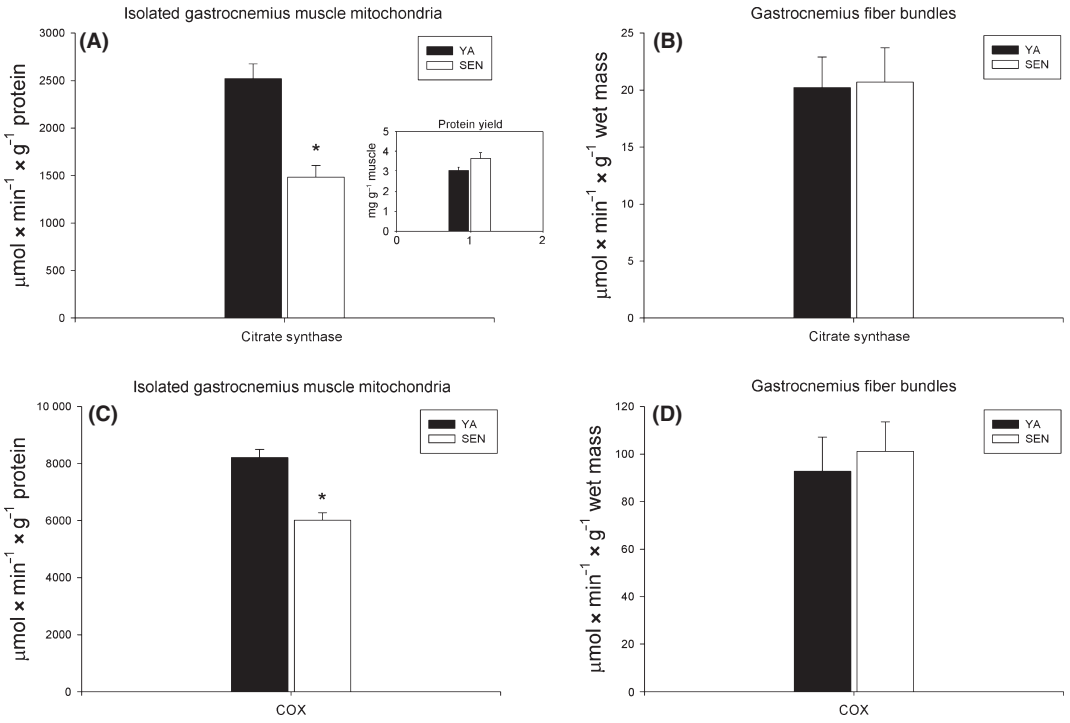

Fig. 1 Mitochondrial enzyme activity is lower with aging in isolated mitochondrial preparations but not in permeabilized fiber bundles. (A) Comparison of citrate synthase (CS) activity measured biochemically from gastrocnemius muscle isolated mitochondria of young adult (YA) and senescent (SEN) rats. The inset represents protein yield recovered from mitochondrial isolation procedures in YA and SEN. (B) Comparison of CS activity measured from permeabilized bundles of YA and SEN gastrocnemius muscles. (C) Comparison of complex IV activity (COX) measured biochemically from isolated mitochondria homogenates. (D) COX activity measured from permeabilized bundles. Enzyme activities for the fiber bundles are reported for the bundles used in H_2O_2 emission experiments and are similar to results obtained in bundles used for respirometry. *$P < 0.05$ vs. YA. COX, cytochrome c oxidase.

I, II, III and IV was 47–69% lower in SEN vs. YA isolates, whereas protein content of subunit alpha of complex V was not different between YA and SEN isolates (Fig. 2). Median mitochondrial particle volume was greater in SEN (Fig. S1C), and median mitochondrial particle Mitotracker Red intensity was lower in SEN mitochondria (Fig. S1D).

Mitochondrial respiration

Representative raw tracings of respirometry experiments are shown in Fig. S2 (Supporting information). Respiratory control ratio (State III GM/GM) in both the isolated mitochondria and the permeabilized bundles showed the preparations to be of high quality (Fig. 3A,B insets) (Frezza *et al.*, 2007b; Kuznetsov *et al.*, 2008). Similar to the biochemical activities noted earlier, the isolated mitochondria from SEN animals exhibited rates of respiration that were 40–60% lower than in YA (Fig. 3A), whereas only *N*,*N*,*N*′,*N*′-tetramethyl-*p*-phenylenediamine (TMPD)-supported respiration was lower in fiber bundles of SEN vs. YA (Fig. 3B). As expected, normalizing for COX activity eliminated the difference in TMPD-driven respiration (direct stimulation of complex IV), but the other differences between YA- and SEN-isolated mitochondria remained (Fig. 3C). Similarly, normalization to COX activity in fiber bundles eliminated

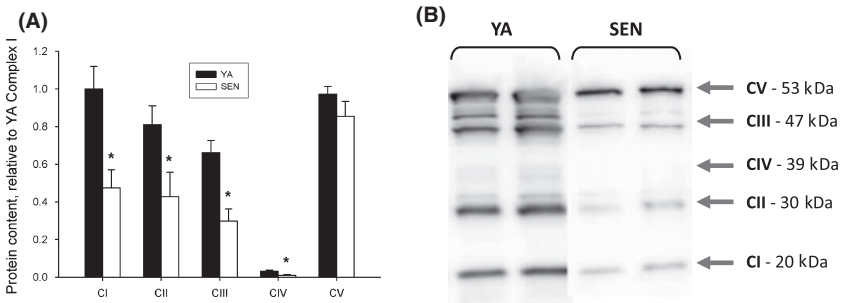

Fig. 2 Mitochondrial protein content is lower in senescent (SEN) mitochondrial isolates. (A) Comparison of the relative content of electron transport chain complexes subunits in young adult (YA)- and SEN-isolated mitochondria. Values are expressed relative to protein content of complex I in YA. (CI: complex I; CII: complex II, CIII: complex III; CIV: complex IV; CV: complex V). (B) Representative Western blots of isolated mitochondria probed for subunits of each ETC. complex. *$P < 0.05$ vs. YA.

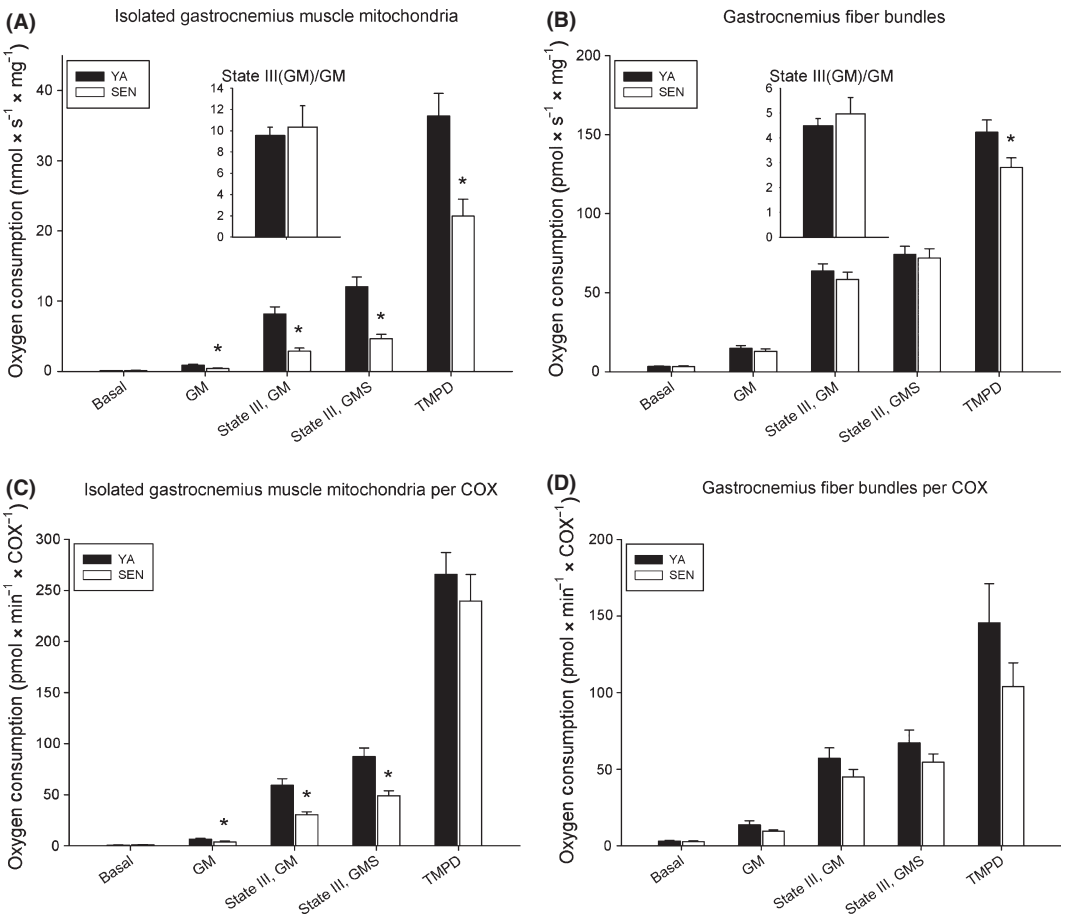

Fig. 3 Mitochondrial respiration is lower with aging in isolated mitochondria, but not in permeabilized fiber bundles. (A) Comparison of O_2 flux measured in isolated gastrocnemius muscle mitochondria from young adult (YA) and senescent (SEN) rats expressed per mg of mitochondrial proteins. Mitochondrial substrates were sequentially added: 10 mM glutamate + 2 mM malate (GM), 2 mM adenosine di-phosphate (State III), 10 mM succinate (GMS), then 10 μM antimycin A followed by 0.5 mM TMPD + 5 mM ascorbate (TMPD). (B) Comparison of oxygen flux measured in permeabilized bundles of YA and SEN gastrocnemius muscles expressed per mg of wet weight. Identical conditions as in A. (C) Oxygen flux in isolated mitochondria normalized per cytochrome c oxidase (COX) activity. (D) Oxygen flux in permeabilized bundles normalized per COX activity. *$P < 0.05$ vs. YA. TMPD, *N*,*N*,*N*′,*N*′-tetramethyl-*p*-phenylenediamine.

the difference in TMPD-driven respiration between YA and SEN (Fig. 3D).

Mitochondrial H_2O_2 emission

The results for H_2O_2 emission from isolated mitochondria were very similar to respiration results in that H_2O_2 emission was markedly lower in SEN than YA mitochondria for all states where substrates were present (Fig. 4A), whereas there were no detectable differences between age-groups in fiber bundles (Fig. 4B). Normalization for COX activity eliminated all differences between YA and SEN mitochondria, except H_2O_2 emission with succinate and under conditions of complex III blockade by antimycin A (AA), which remained lower in the SEN mitochondria (Fig. 4C). On the other hand, normalization for COX activity had no impact on the lack of differences in H_2O_2 emission between age-groups in fiber bundles (Fig. 4D). When expressed per O_2 flux, H_2O_2 release in SEN-isolated mitochondria was similar to YA under basal and glutamate–malate conditions, but was 58% greater under State III respiration compared to YA (Fig. 4E). There was no significant age difference in H_2O_2 release after normalizing for O_2 flux in permeabilized bundles (Fig. 4F). In isolated mitochondria, blocking electron flow at complex III with AA following State III conditions resulted in a 39-fold increase in H_2O_2 release per unit of O_2 flux in YA, compared to a 15-fold increase in SEN. In permeabilized bundles, complex III blockade following State III conditions resulted in a 20-fold increase in YA, compared to an 11-fold increase in SEN. Despite these differences in the extent of increase in H_2O_2 per unit of O_2 flux under these conditions, this did not result in a significant difference in net H_2O_2 emission per unit of O_2 flux between YA and SEN groups in either preparation following AA treatment.

Mitochondrial calcium retention capacity

Isolated mitochondria from SEN exhibited a 39% lower Ca^{2+} retention capacity (CRC) vs. YA mitochondria (Fig. 5A), whereas

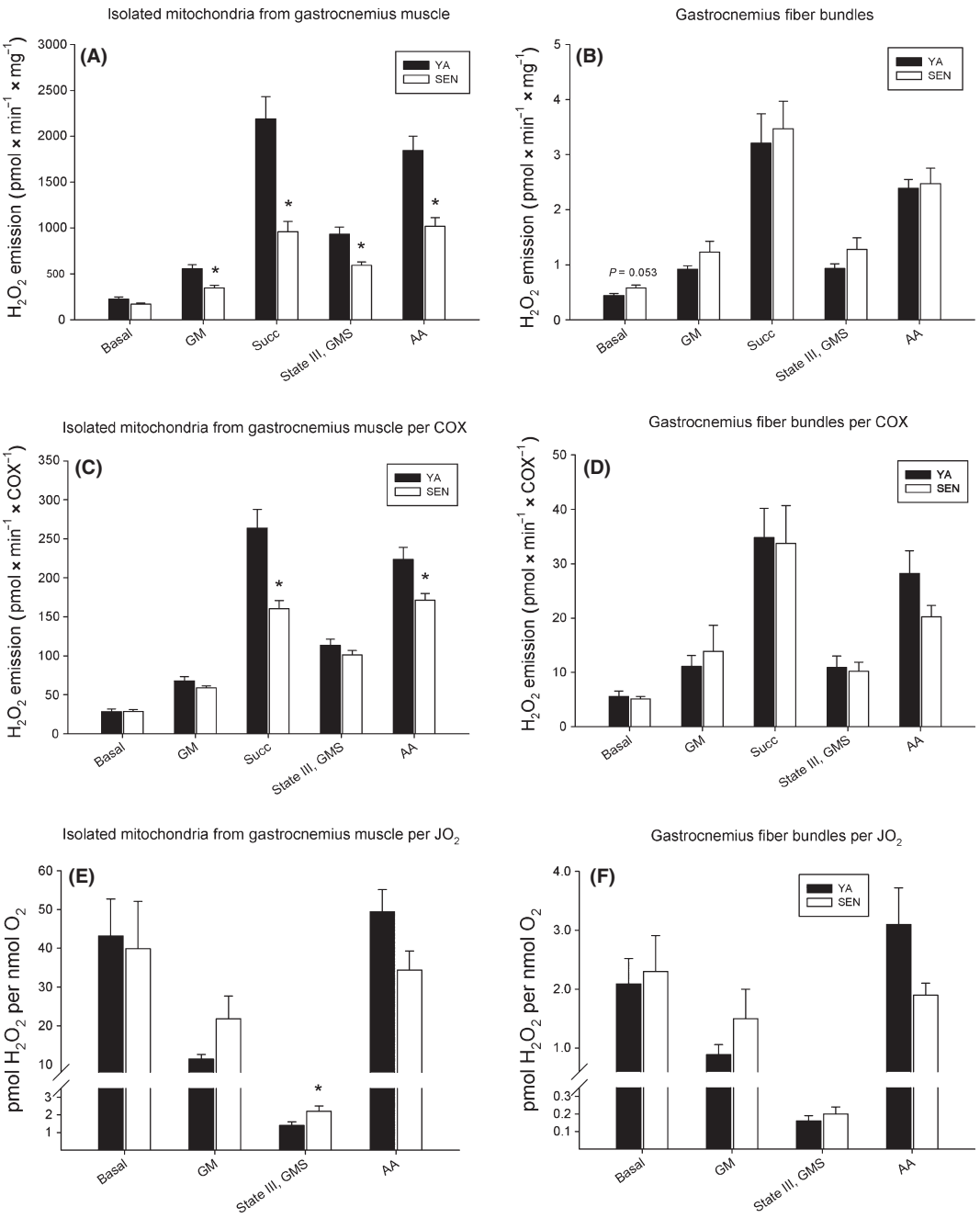

Fig. 4 Mitochondrial H_2O_2 emission is higher with aging in isolated mitochondria, but not in fiber bundles. (A) Comparison of H_2O_2 emission measured in isolated gastrocnemius muscle mitochondria from young adult (YA) and senescent (SEN) rats expressed per mg of proteins. Mitochondrial substrates were sequentially added: 2.5 mM malate + 10 mM glutamate (GM), 10 mM succinate (SUCC), 1 mM adenosine di-phosphate (State III, GMS), then 10 μM antimycin A. (B) H_2O_2 emission measured in permeabilized bundles of YA and SEN gastrocnemius muscles expressed per mg of wet weight. Identical conditions as in A. (C) H_2O_2 emission in isolated mitochondria normalized per cytochrome c oxidase (COX) activity. (D) H_2O_2 emission in permeabilized bundles normalized per COX activity. (E) H_2O_2 emission in isolated mitochondria normalized per oxygen flux from matched respirometry experiments. (F) H_2O_2 emission in permeabilized fiber bundles normalized per oxygen flux. *$P < 0.05$ vs. YA.

there were no differences between age-groups in phantom bundles (Fig. 5B). Normalization for COX activity abolished these differences between YA- and SEN-isolated mitochondria (Fig. 5C) and had no impact on the lack of differences between age-groups in fiber bundles (Fig. 5D).

Time to opening of mPTP

Representative traces of Ca^{2+} uptake and release in isolated mitochondria and phantom fiber bundles of YA (Fig. 6A) and SEN (Fig. 6B) show a significantly shorter time to pore opening

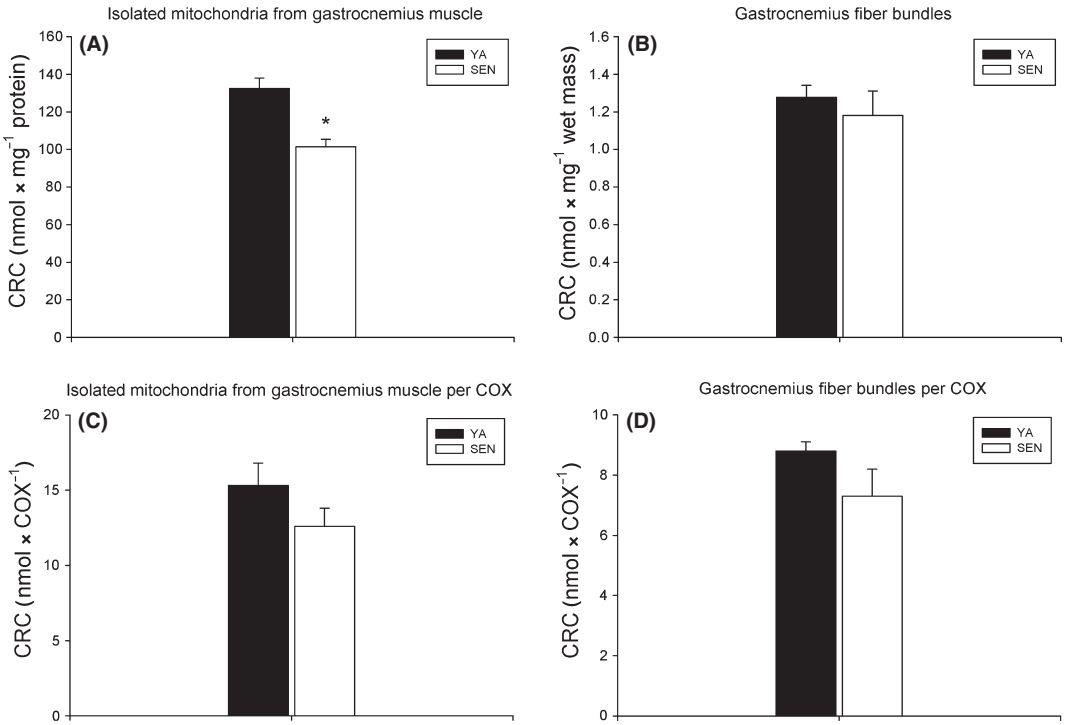

Fig. 5 Calcium retention capacity is unchanged with aging in both isolated mitochondria and permeabilized fibers. (A) Comparison of the amount of Ca^{2+} necessary to trigger opening of the mitochondrial permeability transition pore, or Ca^{2+} retention capacity, measured in isolated gastrocnemius muscle mitochondria of young adult (YA) and senescent (SEN) rats expressed per mg of proteins. About 0.04 mg of protein was added to 1.5 mL of buffer with an initial [Ca^{2+}] of 30 μM. (B) Ca^{2+} retention capacity measured in permeabilized bundles of YA and SEN gastrocnemius muscles expressed per mg of wet weight. About 4–6 mg bundles was added to 600 μL of buffer with an initial [Ca^{2+}] of 30 μM. (C) Ca^{2+} retention capacity in isolated mitochondria normalized per cytochrome c oxidase (COX) activity. (D) Ca^{2+} retention capacity in permeabilized bundles normalized per COX activity. *$P < 0.05$ vs. YA.

in isolated mitochondria (10–20 s) compared to bundles (650–1000 s). In both isolated mitochondria and bundles, there was a shorter time to pore opening in SEN. The mean values of these experiments revealed a 47% shorter time to pore opening in SEN- vs. YA-isolated mitochondria (Fig. 6C) compared to a 29% shorter time to pore opening in SEN vs. YA in phantom bundles (Fig. 6D).

Respiratory and biochemical activity ratios

The integrity of the electron transport chain is reflected in the stoichiometry of respiration rates driven by the different mitochondrial complexes. The ratios of several steps during respiration experiments in isolated mitochondria revealed marked differences in the functional qualities of the mitochondria isolated from SEN vs. YA (Fig. 7A). Specifically, in isolated mitochondria from SEN, we demonstrate higher complex I + II (succinate step) and IV respiration (TMPD step) relative to complex I alone [adenosine di-phosphate (ADP) step; 109% and 168%, respectively] and higher complex IV respiration relative to complex I + II (155%). Similarly, the ratio of COX and CS biochemical activities in SEN was 116% of that of YA. Consistent with many of the other comparisons between isolated mitochondria and fiber bundles, there were no differences in the respiratory or biochemical activity ratios between ages in the fiber bundles (Fig. 7B). Collectively, the respiration and biochemical activity ratios in isolated mitochondria are consistent with a preferential loss of matrix constituents in the SEN age-group during the isolation process.

Discussion

This study provides the first systematic assessment of mitochondrial function in sarcopenic skeletal muscle using two commonly used approaches in parallel: isolated mitochondria (*in vitro*) and permeabilized bundles (*in situ*). Among the differences between these approaches is that whereas mitochondrial isolation disrupts normal mitochondrial interactions and morphology and yields only a fraction of all mitochondria in intact muscle, the permeabilized bundle technique preserves mitochondrial interactions and morphology and provides representation of the totality of the mitochondrial population within muscle (Kuznetsov *et al.*, 2008; Saks *et al.*, 2010). It was on the basis of these differences that we hypothesized that there would be less severe age-related impairments in isolated mitochondria than in fiber bundles because of selective harvest of healthiest mitochondria in isolation procedures. On the contrary, we found that age-related changes were much more severe in isolated mitochondria than permeabilized bundles. In seeking to explain this result, we note that the changes observed with aging in isolated mitochondria were very similar to previous studies showing reduced mitochondrial respiratory capacity (Desai *et al.*, 1996;

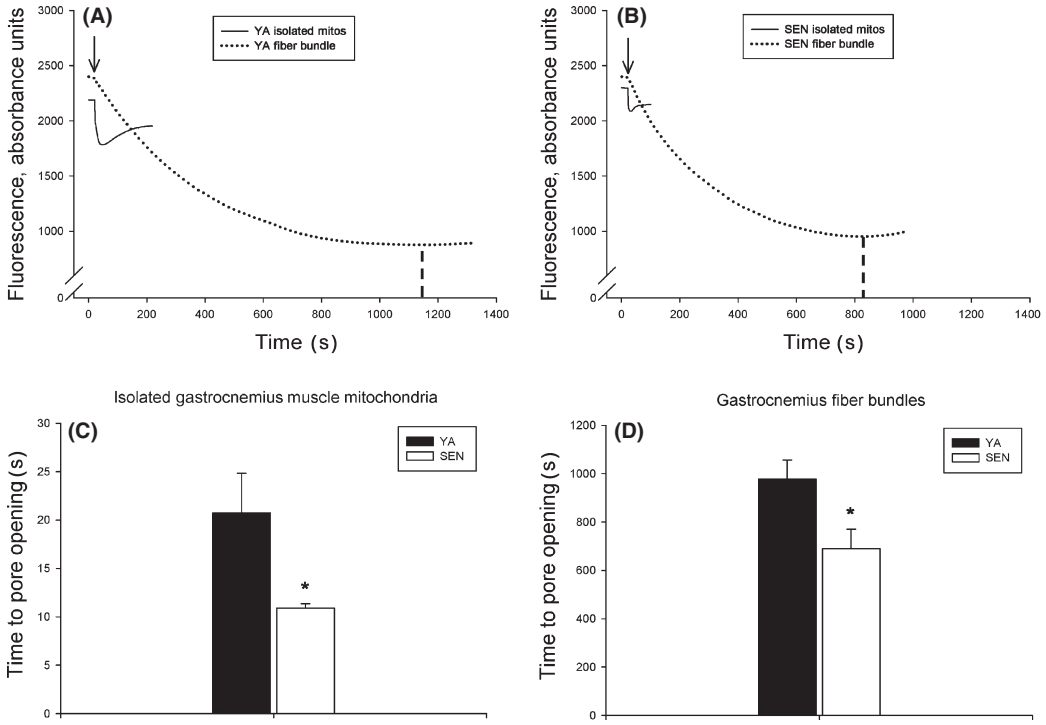

Fig. 6 Mitochondrial permeability transition (mPTP) pore sensitivity to a Ca^{2+} challenge is altered by the mitochondrial isolation process. (A) Representative mitochondrial Ca^{2+}-uptake tracings for isolated mitochondria and permeabilized phantom bundles from young adult (YA) mixed gastrocnemius muscles. Traces show different kinetics for mPTP opening between isolated mitochondria and intact mitochondria in permeabilized fiber bundles. Arrows denote addition of mitochondria or fiber bundles. The dotted vertical line points to the time where mitochondrial Ca^{2+} release induced by the opening of the mPTP caused inversion of the signal and was taken as time to mPTP opening. (B) Representative mitochondrial Ca^{2+} uptake tracings from senescent (SEN) preparations. (C) Comparison of the time to mPTP opening measured in isolated gastrocnemius muscle mitochondria of YA and SEN rats. (D) Time to mPTP opening measured in permeabilized fiber bundles of YA and SEN gastrocnemius muscles. $*P < 0.05$ vs. YA.

Drew *et al.*, 2003; Short *et al.*, 2005), increased ROS generation under some conditions (Capel *et al.*, 2004; Vasilaki *et al.*, 2006; Muller *et al.*, 2007; Chabi *et al.*, 2008), and increased susceptibility of mPTP opening (Chabi *et al.*, 2008; Seo *et al.*, 2008) in mitochondria isolated from aged muscles. On the other hand, we observed relatively mild effects of aging on these indices of mitochondrial function in permeabilized myofiber bundles, and it is this novel observation that sets our results apart from previous studies. It is also important to note that because we used a protease (Nagarse) during our isolation methods, the resulting isolates contain both subsarcolemmal and intermyofibrillar mitochondria (Lanza & Nair, 2009), facilitating comparisons to permeabilized bundles where both mitochondrial populations are present. We conclude that routine mitochondrial isolation procedures yield a markedly exaggerated perception of mitochondrial dysfunction in aged sarcopenic muscle and that mitochondrial functional alterations in aged muscles are much less severe than have been typically considered.

Mitochondrial content in isolated mitochondrial preparations

We used CS activity, a mitochondrial matrix enzyme and recognized marker of mitochondrial volume (Schwerzmann *et al.*, 1989; Picard *et al.*, 2008), and COX activity, an inner mitochondrial membrane-embedded enzyme, to provide estimates of mitochondrial content in our isolated mitochondrial preparations. Our results suggest significantly lower mitochondrial content in SEN- than in YA-isolated mitochondrial preparations. Because CS and COX activities in permeabilized bundles were similar between YA and SEN (Fig. 1B), these results indicate that a lower proportion of mitochondria were extracted from sarcopenic aged muscles despite identical isolation procedures. Consistent with this interpretation, we observed lower absolute amounts of mitochondrial particles in the SEN group with high-resolution confocal microscopy. Efficiency of mitochondrial extraction during the isolation process may be influenced by differences in collagen deposition and connective tissue composition with aging (Goldspink *et al.*, 1994) and/or by the presence of more fragile mitochondrial structures in aged muscles (Piper *et al.*, 1985; Terman & Brunk, 2004). Another possibility is that similar amounts of mitochondrial protein were in fact extracted from the aged muscles during isolation but that a high proportion of these were unable to reconstitute into functional mitochondria and were therefore unable to develop the necessary membrane potential to take up the Mitotracker Red compound. In relation to this point, we note that the amounts of representative subunits of complexes I, II, III and IV detected by Western

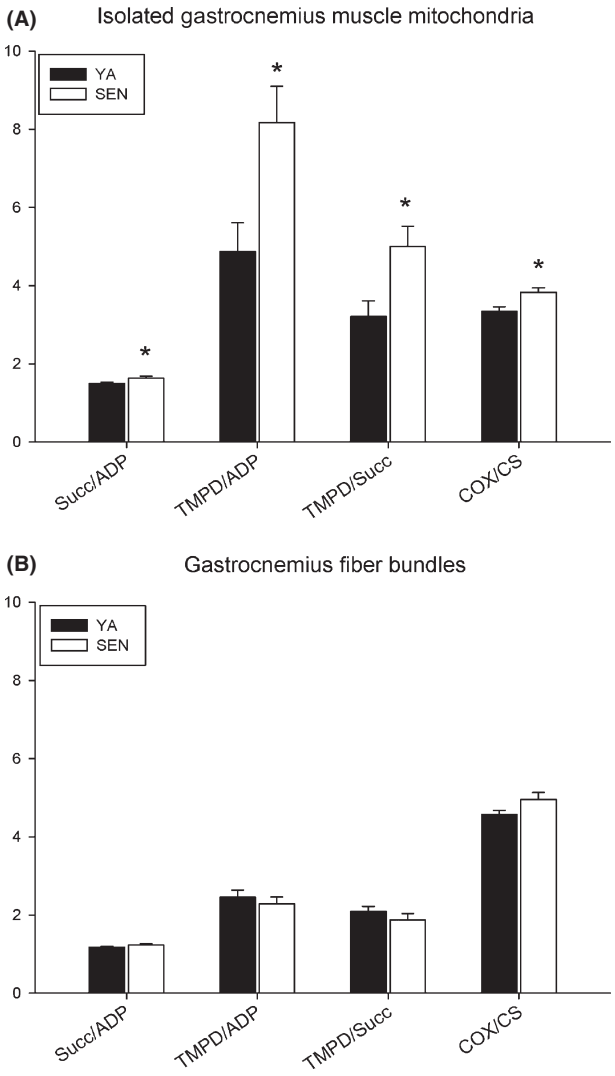

Fig. 7 Respiratory and biochemical activity ratios are altered with aging in isolated mitochondria but not in permeabilized bundles. (A) Comparison of the relative respiratory rates (O_2 flux) measured in isolated gastrocnemius muscle mitochondria of young adult (YA) and senescent (SEN) rats. Oxygen flux was induced by selective activation of complexes of the electron transport chain with GM + ADP (I), GMS + ADP (I + II) and TMPD/ascorbate (IV). Ratios of the respective respiratory activities are shown. Relative biochemical activity of cytochrome c oxidase (COX) (complex IV) and citrate synthase (CS) is also shown. (B) Relative respiratory rates (I + II/I; IV/I; IV/I + II) and biochemical activity (COX/CS) measured in permeabilized bundles of YA and SEN gastrocnemius muscles. $*P < 0.05$ vs. YA. AA, adenosine di-phosphate; TMPD, *N*,*N*,*N*′,*N*′-tetramethyl-*p*-phenylenediamine.

blot in SEN isolates were reduced in similar proportion to the lower mitochondrial particle count seen in Mitotracker Red experiments, suggesting that the primary reason for the lower mitochondrial particle count in SEN isolates was impaired retrieval of mitochondria from SEN muscle during isolation procedures. The basis for the superior yield of complex V vs. the other complexes in SEN isolates is unclear, but may relate to the fact that complexes I, III and IV assemble as supramolecular complexes within the inner mitochondrial membrane and the localization of complexes I, II, III and IV may differ from that of complex V (Schafer *et al.*, 2006; Vonck & Schafer, 2009).

Mitochondrial respiration, H_2O_2 release and sensitivity to mPTP opening

In our study, we chose to examine three indices of mitochondrial function that have relevance to sarcopenia. Specifically, we examined respiratory capacity, H_2O_2 emission, and the sensitivity of the mPTP pore to a Ca^{2+} challenge. We chose these measures because they relate to the decrease in muscle aerobic capacity (Conley *et al.*, 2000; Hagen *et al.*, 2004; Short *et al.*, 2005), increased oxidative damage (Mecocci *et al.*, 1999; Cao *et al.*, 2001; Aiken *et al.*, 2002; Bua *et al.*, 2002; McKenzie *et al.*, 2002; Mansouri *et al.*, 2006), and increased apoptosis (Strasser *et al.*, 2000; Dirks & Leeuwenburgh, 2002; Rice & Blough, 2006) frequently reported in aged skeletal muscles. Whereas our results in isolated mitochondria are similar to many previous studies showing an apparent reduction in respiratory capacity per mitochondrion in aged muscles (Trounce *et al.*, 1989; Kumaran *et al.*, 2005; Chabi *et al.*, 2008), our results in permeabilized myofibers show only a small reduction in complex IV-driven respiration with aging (Fig. 4). Interestingly, normalization of respiration in isolated mitochondrial preparations to COX activity brought the SEN values closer to YA, consistent with the idea that some of the difference we observed between YA- and SEN-isolated mitochondrial preparations was because of lower mitochondrial content in the isolates yielded from SEN muscle. However, age-related differences still remained in the isolates that were not seen in the permeabilized bundles, which we conclude must be an artifact of the isolation procedure. In this respect, our confocal imaging results showed lower mean fluorescence intensity per mitochondrial particle in SEN mitochondria. As the Mitotracker probe is taken up in proportion to mitochondrial membrane potential, our results suggest the lower respiratory capacity of SEN-isolated mitochondria after normalizing for COX activity may be related to a lower membrane potential. Further to this point, we also note that the median mitochondrial particle size was greater in SEN isolates, suggesting greater swelling than is typically associated with isolation procedures (Schwerzmann *et al.*, 1989; Figueiredo *et al.*, 2008) in SEN mitochondria, which could adversely affect the maintenance of mitochondrial membrane potential.

Oxidative phosphorylation and electron transport within the mitochondria are associated with ROS production and H_2O_2 release (Stowe & Camara, 2009), which not only trigger important signaling pathways but can also cause molecular damage and lead to nuclear apoptosis at high levels (St-Pierre *et al.*, 2006; Stowe & Camara, 2009). When expressed per unit O_2 flux, we find that H_2O_2 release from isolated mitochondria is greater in SEN under conditions of maximal respiration (State III, GMS), but we find no significant differences in H_2O_2 release between YA and SEN in permeabilized bundles. Therefore, although our data in isolated mitochondria are consistent with several reports indicating higher ROS production from aged mitochondria (Capel *et al.*, 2004; Mansouri *et al.*, 2006; Chabi *et al.*, 2008), our data suggest that this effect of aging may be limited to, or at least exaggerated by, the mitochondrial isolation

approach. On the other hand, we note that the H_2O_2 emission we report reflects the combined effects of superoxide production, the rate of its conversion to H_2O_2 by superoxide dismutase, and finally, the binding of H_2O_2 to the Amplex red probe to form resorufin. In this respect, recent work indicates that glutathione peroxidases compete with the Amplex Red probe and therefore leads to an underestimate of superoxide production via this method (Treberg *et al.*, 2010). As we have previously reported a doubling of glutathione peroxidase activity in vastus lateralis muscle of SEN F344BN rats previously (Thomas *et al.*, 2010), which is a muscle of similar fiber type to the gastrocnemius muscle (Armstrong & Phelps, 1984), the magnitude of any increase in mitochondrial ROS production with aging would be concealed by an up-regulation of glutathione peroxidase or other antioxidant enzymes. Furthermore, if the amount of glutathione peroxidase enzyme, which is located in the mitochondrial matrix, is reduced as a result of the mitochondrial isolation procedure, this could account for the differences in H_2O_2 emission seen with aging between isolated mitochondria and permeabilized bundles.

Because apoptosis has been strongly implicated in sarcopenia (Siu, 2009), with many studies showing evidence of increased apoptotic activation in aged muscle (Dirks & Leeuwenburgh, 2002; Phillips & Leeuwenburgh, 2005; Siu *et al.*, 2005; Baker & Hepple, 2006; Rice & Blough, 2006), we investigated one of the most potent triggers for apoptosis: mitochondrial outer membrane permeabilization. Physiologically, mitochondrial outer membrane permeabilization is triggered by mPTP opening and is an irreversible event associated with the release of pro-apoptotic factors by the mitochondria (Rasola & Bernardi, 2007). Our result showing an increased sensitivity of mPTP opening to a Ca^{2+} challenge in isolated mitochondria with aging is consistent with recent data using the same animal model and ages as studied here (Chabi *et al.*, 2008; Seo *et al.*, 2008).

In our study, mitochondrial outer membrane permeabilization kinetics assessed by time to mPTP opening demonstrate a more pronounced increase in mPTP sensitivity with age in isolated mitochondria than in permeabilized bundles, leading to an exaggerated impression of susceptibility to apoptosis in aged isolated mitochondria. Furthermore, isolated mitochondria from both YA and SEN groups display a dramatic hypersensitivity to Ca^{2+} compared to permeabilized bundles. As under physiologic conditions mitochondrial outer membrane permeabilization and apoptotic signaling is enhanced by mitochondrial fragmentation (Arnoult, 2007; Detmer & Chan, 2007; Ong *et al.*, 2010) and prevented by mitochondrial fusion (Frezza *et al.*, 2007a), differences in mPTP sensitivity between preparations may be secondary to mechanical fragmentation of mitochondria during isolation. Consistent with this premise, we demonstrate that mitochondrial isolation mechanically fragments mitochondria into small spherical particles, that this phenomenon is associated with marked sensitization of isolated organelles to mPTP opening compared to permeabilized bundles, and that this sensitization effect is more pronounced in the SEN-isolated mitochondria. As such, like the indices of respiratory capacity and ROS production, our results in permeabilized bundles indicate less severe alterations in the function of the mPTP in aging muscle than has been previously suggested.

Qualitative differences between isolated mitochondria and permeabilized bundles

An important consideration in the present study relates to the preferential loss of CS (soluble in matrix) compared to COX (inner mitochondrial membrane-anchored) with aging in the isolated mitochondrial preparation (41% vs. 29% lower in SEN, respectively). This suggests that the marked impairment of mitochondrial respiration and altered H_2O_2 release with aging in isolated mitochondria but not permeabilized bundles may be in part because of a selective loss of mitochondrial matrix constituents during the isolation process owing to transient rupture/resealing of the outer and inner mitochondrial membranes (Schwerzmann *et al.*, 1989), particularly in the aged mitochondrial preparations. Selective loss of matrix enzymes (Krebs cycle enzymes) and metabolic intermediates (nicotinamide adenine nucleotide, NAD^+; flavin adenine dinucleotide, FAD^+) essential for complex I and complex II respiration or antioxidant capacity (e.g., glutathione peroxidase) would certainly influence results from respiration and H_2O_2 assays, and possibly other aspects of mitochondrial function.

To provide insight into this possibility, mitochondrial respiration was sequentially stimulated to allow assessment of the relative activity of different complexes of the electron transport chain. Notably, complex IV activity was directly stimulated by TMPD and therefore independent of mitochondrial matrix enzymes and of electron transport by upstream complexes. In SEN- vs. YA-isolated mitochondria only, we demonstrate higher complex IV activity relative to complex I and complexes I + II operating together. As mentioned earlier, loss of matrix enzymes necessary to convert substrates for mitochondrial respiration and produce reducing equivalents (NADH, $FADH_2$) would selectively reduce complex I- and II-driven respiration. Moreover, this isolation effect is exaggerated in SEN-isolated mitochondria, suggesting that mitochondria from SEN muscles are more likely to lose matrix content. Also, note that the relative amount of subunits from complex I and complex II was proportionally greater than complex IV in SEN isolates when probed by Western blot, showing that this altered respiratory stoichiometry is not because of lower protein levels of complexes I and II in SEN isolates. Collectively, our findings indicate that mitochondrial isolation procedures induce specific alterations of mitochondrial respiration in aged muscle mitochondria that are not seen *in situ* and that this effect is likely in part because of greater loss of matrix constituents during isolation in SEN mitochondria.

Conclusions

Taken together, our findings clearly establish that isolated muscle mitochondria exhibit exaggerated impairments with aging

when compared with permeabilized muscle bundles. Although some of this effect is attributable to differences in mitochondrial content between YA- and SEN-isolated mitochondrial preparations, we also show important qualitative differences in mitochondrial morphology and function, which are independent of mitochondrial content. In contrast, our results in permeabilized myofibers reveal only a minor defect in mitochondrial respiratory capacity, no change in ROS emission (although an increase in glutathione peroxidase activity with aging likely conceals an increase in ROS), and a mild increase in sensitivity of the mPTP to opening in SEN skeletal muscle. As such, our results indicate that changes in mitochondrial function in aged sarcopenic skeletal muscle are less severe than typically indicated from isolated organelle studies.

One interpretation of our results is that mitochondrial isolation may reveal weaknesses within the mitochondrial machinery that are present but not evident *in vivo* or in permeabilized bundles (*in situ*). This warrants caution in directly translating putative weaknesses observed in isolated mitochondria to physiologically relevant dysfunction *in vivo*. On the other hand, these *in vitro* preparations may nevertheless be useful in the context of aging to study key aspects of mitochondrial biology given further understanding of how the isolation procedures affect mitochondrial structure and composition. In particular, we suggest that the isolation of mitochondria represents an intervention that can be used to facilitate the study of mitochondrial resilience and stress resistance, whereas the permeabilized bundle method is better suited to provide insight into the day-to-day function of mitochondria. On this basis, while our results *in situ* suggest mitochondrial function is relatively well preserved in sarcopenic muscle, our results also demonstrate that aged mitochondria have a markedly impaired ability to tolerate the stress of isolation, which may provide physiologically relevant insight into the ability of aged mitochondria to tolerate stress in general.

Experimental procedures

Animals and surgical methods

All procedures were conducted with approval from the University of Calgary Animal Care Committee. Male Fischer 344 × Brown Norway F1-hybrid (F344BN) rats were obtained from the colony maintained by the National Institute on Aging at ages of 8–10 months (YA) and 35–36 months (SEN). The ages were chosen to represent a period where there is substantial age-related muscle atrophy and dysfunction (Brown & Hasser, 1996; Hagen *et al.*, 2004; Hepple *et al.*, 2004) and thus to permit insight into changes that would be relevant to sarcopenia. Upon arrival at our institution, rats were housed individually in cages fitted with filter bonnets at the University of Calgary Biological Sciences vivarium and were kept a minimum of 48 h prior to being used in experiments (12:12 h light/dark cycle, ambient temperature 23 °C). Food and water were provided *ad libitum*.

On the day of experiment, rats were anesthetized with 55–65 mg kg^{-1} sodium pentobarbital (i.p.). The left and right gastrocnemius (Gas) muscles from eight YA and eight SEN animals were carefully dissected and placed into ice-cold stabilizing Buffer A [in mM: 2.77 CaK_2 Ethylene glycol-bis(2-aminoethylether)-N,N,N′,N′-tetraacetic acid (EGTA), 7.23 K_2 EGTA, 6.56 $MgCl_2$, 0.5 dithiothreitol (DTT), 50 2-(N-morpholino)ethanesulfonic acid potassium salt (K-MES), 20 imidazol, 20 taurine, 5.3 Na_2 ATP, 15 phosphocreatine, pH 7.3 at 4 °C]. To facilitate greater homogeneity between samples obtained from a given Gas muscle, the highly oxidative red region and highly glycolytic white region of this muscle were removed to leave the mixed region of this muscle. The mixed Gas was then divided equally for mitochondrial isolation and permeabilized myofiber preparations.

Mitochondrial isolation

Mitochondrial isolation was performed using standard homogenization, protease digestion and differential centrifugation methods, similar to those described by (Frezza *et al.*, 2007b). Mixed gas was weighed and placed in 20 mL of ice-cold mitochondrial extraction buffer (in mM: 100 sucrose, 50 KCl, 5 EDTA, 2 KH_2PO_4, 50 Tris-base, pH 7.4 at 4 °C) and subsequently minced manually with fine scissors. All steps were performed at 4 °C. Minced tissue was homogenized at 600 rpm with a motor-driven Teflon Potter Elvehjem pestle (Corning Inc., Lowell, MA, USA) (six up and down pulses), incubated with 1 mg g^{-1} Nagarse protease (P8038; Sigma-Aldrich, Oakville, ON, Canada) for 5 min, diluted further with another 20 mL extraction buffer and homogenized again at 600 rpm (four up and down pulses). The homogenate was centrifuged at 1000 *g* for 10 min, after which the mitochondria-rich supernatant was filtered through cheesecloth and the pellet discarded. Mitochondria were then pelleted by centrifugation at 8000 *g* for 10 min and gently re-suspended in re-suspension buffer (in mM: 100 sucrose, 50 KCl, .05 EDTA, 2 KH_2PO_4, 50 Tris-base, pH 7.4 at 4 °C), centrifuged again at 8000 *g* for 10 min, and the final pellet gently re-suspended in 600 μL of re-suspension buffer. Mitochondrial protein concentration was measured spectrophotometrically using the bicinchoninic acid assay (23225; Thermo Scientific, Waltam, MA, USA). Isolated mitochondria were used fresh for functional measurements. A portion of fresh isolated mitochondria was frozen for Western blots and enzymatic activity measurements.

Preparation of permeabilized myofiber bundles

Dissection and permeabilization of myofiber bundles with saponin was performed according to methods described by Kuznetsov *et al.* (Kuznetsov *et al.*, 2008) and as we have described previously (Picard *et al.*, 2008). After dissection, muscles were immediately put on ice in precooled (4 °C) Buffer A (described previously) and weighed. Whole muscles were trimmed of connective tissue and manually teased into small fiber bundles. Once dissection was completed, fiber bundles were placed in

Buffer A supplemented with 0.05 mg mL^{-1} saponin to allow selective permeabilization of the sarcolemma. Following 30 min of incubation at low rocking speed, fiber bundles were subjected to 3 × 10 min rinses in Buffer B (in mM: 2.77 CaK_2 EGTA, 7.23 K_2 EGTA, 1.38 $MgCl_2$, 3.0 K_2HPO_4, 0.5 DTT, 20 imidazole, 100 K-MES, 20 taurine, pH 7.3, at 4 °C) supplemented with fatty acid-free bovine serum albumin (BSA: 2 mg mL^{-1}). Fiber bundles for respiration experiments were kept in Buffer B on ice until use.

High-resolution respirometry

Permeabilized myofiber and isolated mitochondrial respiration were assessed with a polarographic oxygen sensor (Oxygraph-2k, Oroboros, Innsbruck, Austria) calibrated as required for O_2 concentration, environmental variables, and auto O_2 consumption. Briefly, 3.5–6 mg (wet weight) permeabilized bundles or 0.01 mg mitochondrial protein, prepared as described earlier, was added to 2 mL of Buffer B in the respirometer and equilibrated for baseline endogenous respiration at 37 °C. Myofiber respiration was performed at hyperoxygenated levels to eliminate O_2 diffusion limitations. The substrate protocol assessing O_2 flux was added sequentially as follows, with each step interspersed with a period of stabilization between injections: 10 mM glutamate + 2 mM malate (GM), 2 mM ADP, 10 μM succinate (SUCC), 10 μM cytochrome c, 10 μM AA, 5 mM ascorbate + 0.5 mM TMPD. To account for TMPD auto-oxidation, rates of TMPD oxidation were initially determined at different O_2 concentrations without samples present. Auto-oxidation-associated respiration was then subtracted from TMPD respiration values obtained in the presence of samples. After respiration measurements were completed, bundles were removed and placed in liquid N_2 and stored at −80 °C for enzymatic measures. Respiration was expressed as picomoles per second per mg wet weight for bundles, per mg protein for isolated mitochondria, and as nanomoles per enzymatic unit (U) of cytochrome oxidase activity for both preparations.

ROS emission

Reactive oxygen species emission was detected by measuring the rate of appearance of resorufin from Amplex Red with a Hitachi (Hitachi High Technologies Canada Inc., Rexdale, ON, Canada) F-2500 fluorescence spectrophotometer at an excitation/emission wavelength of 563/587 nm, using the FL solutions software. Resorufin is formed by the 1:1 reaction of H_2O_2 and Amplex Red and is catalyzed by horseradish peroxidase. A standard curve was generated daily from the slope of ΔF/min under experimental conditions in the absence of samples and used to calculate the rate of H_2O_2 production. Samples were prepared as described earlier. Permeabilized bundles used for ROS measurement were further washed 3 × 10 min in Buffer Z (in mM: 110 K-MES, 35 KCl, 1 EGTA, 3 $MgCl_2$, 10 K_2HPO_4, pH 7.3 at 4 °C) supplemented with BSA (5 mg mL^{-1}). Bundles (4–6 mg wet weight) or isolated mitochondria (0.01 mg) were added to a thermojacketed, magnetically stirred cuvette containing 600 μL Buffer Z, Amplex Red (5.5 uM), and horseradish peroxidase (1 U mL^{-1}), after a period of baseline autofluorescence. All measures were performed at 37 °C. After the reaction was initiated, substrates were added as follows (allowing a period of stabilization between each step): GM (10 + 2 mM), SUCC (10 mM), ADP (10 μM), ADP (100 μM), ADP (1 mM), AA (10 μM). At the conclusion of the ROS measurements, bundles were placed in liquid N_2 and stored at −80 °C for enzymatic analysis. H_2O_2 emission is expressed as picomoles per minute per mg wet weight for bundles, per mg protein for isolated mitochondria, and as per U of cytochrome oxidase for both preparations.

Biochemical assays for CS and COX

Citrate synthase and COX activity were used as representative of a mitochondrial matrix enzyme and an electron transport chain enzyme, respectively, and to estimate mitochondrial content in each preparation (Schwerzmann *et al.*, 1989). For these measurements, frozen permeabilized bundles used for respirometry and ROS emission assays, and isolated mitochondria frozen immediately after isolation were used. All samples were homogenized in an extraction buffer containing 50 mM triethanolamine and 1 mM EDTA. Permeabilized bundles were finely minced using small scissors and homogenized on ice using a small pestle rotor in 1:20 w/v. Isolated mitochondria were diluted 1:10 v/v, vigorously vortexed, and incubated on ice for 20 min. Citrate synthase activity was measured spectrophotometrically by detecting the increase in absorbance at 412 nm in a 96-well plate at 30 °C, using 200 μL of a reaction buffer (200 mM Tris, pH 7.4) containing (in μM: 2 acetyl-CoA, 200 5,5′-dithiobis-(2-nitrobenzoic acid) (DTNB), 350 oxaloacetic acid, 0.1% Triton-x). Cytochrome c oxidase activity was measured by detecting the decrease in absorbance at 550 nm in a 96-well plate at 30 °C, using 200 μL of a reaction buffer (potassium phosphate 100 mM, pH 7.0) containing 0.1% n-dodecylmaltoside and 0.1 mM purified reduced cytochrome c. The molar extinction coefficients used were 13.6 L mol^{-1} cm^{-1} for DTNB and 29.5 L mol^{-1} cm^{-1} for reduced cytochrome c.

Imaging of isolated mitochondria

Freshly isolated mitochondria were diluted to a protein concentration of about 2.5 mg mL^{-1} (see Fig. 2 for specific values) and incubated with 16.7 μM of Mitotracker Red CMXROS (Molecular Probes M7512, Invitrogen Canada Inc., Burlington, ON, Canada) for 20 min at 30 °C. Ten microliters of labeled mitochondria was placed on a glass slide and mounted with a coverslip to be imaged. Excess liquid was extruded, mitochondria were left to settle for 5 min, and images were acquired using a confocal microscope (Olympus Fluoview FV1000, Olympus fluoview version 2.0c software, Olympus Canada, Markam, ON, Canada) with a PlanApo N 60x/1.42 oil-immersion objective and 1.6 digital zoom (96× final, 1 pixel = 0.0827 μm). Alexa Fluor 546 (Invitrogen Canada Inc., Burlington, ON, Canada) excitation settings

were used with pinhole size of 110 μm, z-slices of 0.5 or 0.3 μm, and the following laser settings: high voltage (HV) = 369, Gain = 1, Offset = 21. Imaris 7.0 software was used to analyze z-stacks and produce surface renderings, volume and mean fluorescence intensity measurements. Software settings were smooth deactivated; diameter of largest sphere of 0.7 μm; threshold for background subtraction of 1030 μm^2; split touching objects enabled; estimated diameter of 0.444 μm; quality threshold above 260; and sphericity threshold above 0.550 (94%+ selection). Representative images were obtained from the microscope's natural perspective (top view) and from the perpendicular perspective (side view) of the 3D surface analysis. Volume and mean fluorescence intensity (independent of particle size) were computed for each individual particle.

Western blotting for electron transport chain composition in isolated mitochondria

Frozen–thawed mitochondrial isolates were used in Western blotting experiments to determine the relative amounts of each of the electron transport chain complexes in each age-group. Briefly, 5 μg of protein was loaded from each isolate into precast 4–15% SDS–polyacrylamide gels (SDS–PAGE) (Bio-Rad, Hercules, CA, USA) and ran for 1.5 h at 110 V. Proteins were then electro-transferred for 1.5 h at 400 mA onto a polyvinylfluoride membrane (PVDF) and incubated overnight with a premixed cocktail of polyclonal antibodies directed against representative subunits of each of the electron transport chain complexes (Mitosciences MS604, 6 μg mL^{-1}, Mitosciences, Eugene, OR, USA). Equal protein loading was verified using the Ponceau red stain. Membranes were washed in 0.05% Tween–PBS buffer and incubated with horseradish peroxidase-conjugated secondary antibody (dilution 1:1000). Signals were detected using the enhanced chemiluminescence detection system (Pierce), and chemiluminescence was digitally captured (Syngene Bio-Imager, Frederick, MD, USA) and densitometry measured using the Bio-imager software (Syngene Tools).

Preparation of phantom fiber bundles

In normal permeabilized myofibers, myosin/actin-associated proteins with high affinity for Ca^{2+} prevent measurements of mitochondrial calcium uptake (Saks *et al.*, 1998; Picard *et al.*, 2008). We therefore prepared phantom fibers without myosin as previously described (Saks *et al.*, 1998). Fiber bundles were first permeabilized with saponin and washed three times in Buffer B as described earlier, then washed three times for 10 min in Buffer C (in mM: K-MES 80, HEPES 50, taurine 20, DTT 0.5, MgCl2 10, ATP 10, pH 7.3 at 4 °C). Fibers where then incubated for 30 min with intermittent manual agitation at 4 °C in Buffer D (in mM: KCl 800, HEPES 50, taurine 20, DTT 0.5, $MgCl_2$ 10, ATP 10, pH 7.3 at 4 °C), a solution of high ionic force to extract myosin but which preserves mitochondrial function (Picard *et al.*, 2008). Bundles were then washed three times in low-EGTA CRC Buffer (in mM: 250 sucrose, 10 Tris, 0.005 EGTA, 10 3-(N-morpholino)propane sulphonic acid (MOPS), pH 7.3 at 4 °C) and kept on ice until use for Ca^{2+}-induced mPTP opening assays.

Sensitivity to Ca^{2+}-induced mPTP opening

Accumulation of Ca^{2+} in the mitochondrial matrix is one of the most important and obligatory triggers for mPTP opening in skeletal muscle (Zoratti & Szabo, 1995). Sensitivity to mPTP opening is therefore commonly assessed in isolated mitochondria by determining mitochondrial CRC in the presence of a Ca^{2+} challenge (Ichas *et al.*, 1994). In the present study, a novel method recently developed by Picard *et al.* was used to determine CRC in permeabilized phantom fibers (Picard *et al.*, 2008). Briefly, a muscle bundle of 4–6 mg wet weight was added to 600 μL of CRC Buffer containing about 30 μM of Ca^{2+} supplemented with (in mM: 5 glutamate, 2.5 malate, 10 Pi, 0.001 Calcium-green 5 N and 0.5 nM oligomycin). For isolated mitochondria, about 0.04 mg of proteins was added to 1.5 mL of the same buffer. Mitochondrial Ca^{2+} uptake was immediately followed by monitoring the decrease in extra-mitochondrial Ca^{2+} concentration using the fluorescent probe Calcium-green 5 N (Molecular Probes). Fluorescence was detected using a spectrophotometer (Hitachi Fluoroscence Spectrophotometer F2500, FL Solutions software) with excitation and emission detectors set at 505 and 535 nm, respectively. We have previously demonstrated that this phenomenon is mitochondrial-specific and responsive to the inhibitor of the mPTP, cyclosporine A (Picard *et al.*, 2008). Progressive uptake of Ca^{2+} by mitochondria was monitored until mitochondrial Ca^{2+} release caused by opening of the mPTP was observed as the inversion of signal. Ca^{2+} retention capacity, a reliable index of mPTP sensitivity (Csukly *et al.*, 2006), was calculated as total amount of Ca^{2+} taken by mitochondria prior to Ca^{2+} release. For all isolated mitochondria assays, a fixed amount of Ca^{2+} was subtracted from the drop in signal to account for intrinsic Ca^{2+} buffering capacity of the re-suspension buffer. Ca^{2+} retention capacity values were expressed per mg of wet fiber weight for bundles, per mg of proteins for isolated mitochondria, and per U of COX.

Statistical analyses

All values are presented as means ± standard error (SEM). Two-tailed student's *T* test assuming unequal variance was used to determine *P* values. *P* value = 0.05 was considered significant. To account for unequal sample size in the analysis of isolated mitochondria median particle size and fluorescence intensity (Fig. S1), a Mann–Whitney rank sum test was used to determine *P* values.

Acknowledgments

This work was supported by operating grants from the Canadian Institutes for Health Research (MOP 57808 and IAO 84673 to RTH). The authors thank Dr. Yan Burelle for valuable discussion of the data.

Author contributions

RTH and MP designed the experiments, which were performed by MP, DR, and KJW. Animal surgery was performed by MMT and assisted by SLR. CR ran the Western blots. The data were analyzed by MP, RTH, and DR. The confocal imaging experiments and analysis were carried out by MP. RTH and MP interpreted the data, and the manuscript was written by RTH, MP, TT, and DR.

References

Aiken J, Bua E, Cao Z, Lopez M, Wanagat J, McKenzie D, McKiernan S (2002) Mitochondrial DNA deletion mutations and sarcopenia. *Ann. N Y Acad. Sci.* **959**, 412–423.

Alway SE, Degens H, Krishnamurthy G, Smith CA (2002) Potential role for Id myogenic repressors in apoptosis and attenuation of hypertrophy in muscles of aged rats. *Am. J. Physiol. Cell Physiol.* **283**, C66–C76.

Armstrong RB, Phelps RO (1984) Muscle fiber type composition of the rat hindlimb. *Am. J. Anat.* **171**, 259–272.

Arnoult D (2007) Mitochondrial fragmentation in apoptosis. *Trends Cell Biol.* **17**, 6–12.

Bakeeva LE, Chentsov Yu S, Skulachev VP (1978) Mitochondrial framework (reticulum mitochondriale) in rat diaphragm muscle. *Biochim. Biophys. Acta* **501**, 349–369.

Baker DJ, Hepple RT (2006) Elevated caspase and AIF gene expression correlate with progression of sarcopenia during aging in male F344BN rats. *Exp. Gerontol.* **41**, 1149–1156.

Benard G, Bellance N, James D, Parrone P, Fernandez H, Letellier T, Rossignol R (2007) Mitochondrial bioenergetics and structural network organization. *J. Cell Sci.* **120**, 838–848.

Brown M, Hasser EM (1996) Complexity of age-related change in skeletal muscle. *J. Gerontol. A Biol. Sci. Med. Sci.* **51**, B117–B123.

Bua EA, McKiernan SH, Wanagat J, McKenzie D, Aiken JM (2002) Mitochondrial abnormalities are more frequent in muscles undergoing sarcopenia. *J. Appl. Physiol.* **92**, 2617–2624.

Cao Z, Wanagat J, McKiernan SH, Aiken JM (2001) Mitochondrial DNA deletion mutations are concomitant with ragged red regions of individual, aged muscle fibers: analysis by laser-capture microdissection. *Nucleic Acids Res.* **29**, 4502–4508.

Capel F, Buffiere C, Patureau Mirand P, Mosoni L (2004) Differential variation of mitochondrial H2O2 release during aging in oxidative and glycolytic muscles in rats. *Mech. Ageing Dev.* **125**, 367–373.

Chabi B, Ljubicic V, Menzies KJ, Huang JH, Saleem A, Hood DA (2008) Mitochondrial function and apoptotic susceptibility in aging skeletal muscle. *Aging Cell* **7**, 2–12.

Conley KE, Jubrias SA, Esselman PC (2000) Oxidative capacity and ageing in human muscle. *J. Physiol.* **526**(Pt 1), 203–210.

Csukly K, Ascah A, Matas J, Gardiner PF, Fontaine E, Burelle Y (2006) Muscle denervation promotes opening of the permeability transition pore and increases the expression of cyclophilin D. *J. Physiol.* **574**, 319–327.

Desai VG, Weindruch R, Hart RW, Feuers RJ (1996) Influences of age and dietary restriction on gastrocnemius electron transport system activities in mice. *Arch. Biochem. Biophys.* **333**, 145–151.

Detmer SA, Chan DC (2007) Functions and dysfunctions of mitochondrial dynamics. *Nat. Rev. Mol. Cell Biol.* **8**, 870–879.

Dirks A, Leeuwenburgh C (2002) Apoptosis in skeletal muscle with aging. *Am. J. Physiol. Regul. Integr. Comp. Physiol.* **282**, R519–R527.

Drew B, Phaneuf S, Dirks A, Selman C, Gredilla R, Lezza A, Barja G, Leeuwenburgh C (2003) Effects of aging and caloric restriction on mitochondrial energy production in gastrocnemius muscle and heart. *Am. J. Physiol. Regul. Integr. Comp. Physiol.* **284**, R474–R480.

Figueiredo PA, Ferreira RM, Appell HJ, Duarte JA (2008) Age-induced morphological, biochemical, and functional alterations in isolated mitochondria from murine skeletal muscle. *J. Gerontol. A Biol. Sci. Med. Sci.* **63**, 350–359.

Figueiredo PA, Powers SK, Ferreira RM, Amado F, Appell HJ, Duarte JA (2009) Impact of lifelong sedentary behavior on mitochondrial function of mice skeletal muscle. *J. Gerontol. A Biol. Sci. Med. Sci.* **64**, 927–939.

Frezza C, Cipolat S, Scorrano L (2007a) Measuring mitochondrial shape changes and their consequences on mitochondrial involvement during apoptosis. *Methods Mol. Biol.* **372**, 405–420.

Frezza C, Cipolat S, Scorrano L (2007b) Organelle isolation: functional mitochondria from mouse liver, muscle and cultured fibroblasts. *Nat. Protoc.* **2**, 287–295.

Fugere NA, Ferrington DA, Thompson LV (2006) Protein nitration with aging in the rat semimembranosus and soleus muscles. *J. Gerontol. A Biol. Sci. Med. Sci.* **61**, 806–812.

Goldspink G, Fernandes K, Williams PE, Wells DJ (1994) Age-related changes in collagen gene expression in the muscles of mdx dystrophic and normal mice. *Neuromuscul. Disord.* **4**, 183–191.

Hagen JL, Krause DJ, Baker DJ, Fu MH, Tarnopolsky MA, Hepple RT (2004) Skeletal muscle aging in F344BN F1-hybrid rats: I. Mitochondrial dysfunction contributes to the age-associated reduction in VO2max. *J. Gerontol. A Biol. Sci. Med. Sci.* **59**, 1099–1110.

Hepple RT, Hagen JL, Krause DJ, Baker DJ (2004) Skeletal muscle aging in F344BN F1-hybrid rats: II. Improved contractile economy in senescence helps compensate for reduced ATP generating capacity. *J. Gerontol. A Biol. Sci. Med. Sci.* **59**, 1111–1119.

Hepple RT, Qin M, Nakamoto H, Goto S (2008) Caloric restriction optimizes the proteasome pathway with aging in rat plantaris muscle: implications for sarcopenia. *Am. J. Physiol. Regul. Integr. Comp. Physiol.* **295**, R1231–R1237.

Hiona A, Leeuwenburgh C (2008) The role of mitochondrial DNA mutations in aging and sarcopenia: implications for the mitochondrial vicious cycle theory of aging. *Exp. Gerontol.* **43**, 24–33.

Hutter E, Skovbro M, Lener B, Prats C, Rabol R, Dela F, Jansen-Durr P (2007) Oxidative stress and mitochondrial impairment can be separated from lipofuscin accumulation in aged human skeletal muscle. *Aging Cell* **6**, 245–256.

Ichas F, Jouaville LS, Sidash SS, Mazat JP, Holmuhamedov EL (1994) Mitochondrial calcium spiking: a transduction mechanism based on calcium-induced permeability transition involved in cell calcium signalling. *FEBS Lett.* **348**, 211–215.

Kayar SR, Hoppeler H, Mermod L, Weibel ER (1988) Mitochondrial size and shape in equine skeletal muscle: a three-dimensional reconstruction study. *Anat. Rec.* **222**, 333–339.

Kumaran S, Panneerselvam KS, Shila S, Sivarajan K, Panneerselvam C (2005) Age-associated deficit of mitochondrial oxidative phosphorylation in skeletal muscle: role of carnitine and lipoic acid. *Mol. Cell. Biochem.* **280**, 83–89.

Kuznetsov AV, Veksler V, Gellerich FN, Saks V, Margreiter R, Kunz WS (2008) Analysis of mitochondrial function in situ in permeabilized muscle fibers, tissues and cells. *Nat. Protoc.* **3**, 965–976.

Lanza IR, Nair KS (2009) Functional assessment of isolated mitochondria in vitro. *Methods Enzymol.* **457**, 349–372.

Lecker SH, Jagoe RT, Gilbert A, Gomes M, Baracos V, Bailey J, Price SR, Mitch WE, Goldberg AL (2004) Multiple types of skeletal muscle

atrophy involve a common program of changes in gene expression. *FASEB J.* **18**, 39–51.

Lesnefsky EJ, Hoppel CL (2006) Oxidative phosphorylation and aging. *Ageing Res. Rev.* **5**, 402–433.

Manoli I, Alesci S, Blackman MR, Su YA, Rennert OM, Chrousos GP (2007) Mitochondria as key components of the stress response. *Trends Endocrinol. Metab.* **18**, 190–198.

Mansouri A, Muller FL, Liu Y, Ng R, Faulkner J, Hamilton M, Richardson A, Huang TT, Epstein CJ, Van Remmen H (2006) Alterations in mitochondrial function, hydrogen peroxide release and oxidative damage in mouse hind-limb skeletal muscle during aging. *Mech. Ageing Dev.* **127**, 298–306.

McKenzie D, Bua E, McKiernan S, Cao Z, Aiken JM (2002) Mitochondrial DNA deletion mutations: a causal role in sarcopenia. *Eur. J. Biochem.* **269**, 2010–2015.

Mecocci P, Fano G, Fulle S, MacGarvey U, Shinobu L, Polidori MC, Cherubini A, Vecchiet J, Senin U, Beal MF (1999) Age-dependent increases in oxidative damage to DNA, lipids, and proteins in human skeletal muscle. *Free Radic. Biol. Med.* **26**, 303–308.

Muller FL, Song W, Jang YC, Liu Y, Sabia M, Richardson A, Van Remmen H (2007) Denervation-induced skeletal muscle atrophy is associated with increased mitochondrial ROS production. *Am. J. Physiol. Regul. Integr. Comp. Physiol.* **293**, R1159–R1168.

Ogata T, Yamasaki Y (1997) Ultra-high-resolution scanning electron microscopy of mitochondria and sarcoplasmic reticulum arrangement in human red, white, and intermediate muscle fibers. *Anat. Rec.* **248**, 214–223.

Ong SB, Subrayan S, Lim SY, Yellon DM, Davidson SM, Hausenloy DJ (2010) Inhibiting mitochondrial fission protects the heart against ischemia/reperfusion injury. *Circulation* **121**, 2012–2022.

Phillips T, Leeuwenburgh C (2005) Muscle fiber specific apoptosis and TNF-alpha signaling in sarcopenia are attenuated by life-long calorie restriction. *FASEB J.* **19**, 668–670.

Picard M, Csukly K, Robillard ME, Godin R, Ascah A, Bourcier-Lucas C, Burelle Y (2008) Resistance to Ca2+-induced opening of the permeability transition pore differs in mitochondria from glycolytic and oxidative muscles. *Am. J. Physiol. Regul. Integr. Comp. Physiol.* **295**, R659–R668.

Piper HM, Sezer O, Schleyer M, Schwartz P, Hutter JF, Spieckermann PG (1985) Development of ischemia-induced damage in defined mitochondrial subpopulations. *J. Mol. Cell. Cardiol.* **17**, 885–896.

Rasola A, Bernardi P (2007) The mitochondrial permeability transition pore and its involvement in cell death and in disease pathogenesis. *Apoptosis* **12**, 815–833.

Rice KM, Blough ER (2006) Sarcopenia-related apoptosis is regulated differently in fast- and slow-twitch muscles of the aging F344/N x BN rat model. *Mech. Ageing Dev.* **127**, 670–679.

Romanello V, Guadagnin E, Gomes L, Roder I, Sandri C, Petersen Y, Milan G, Masiero E, Del Piccolo P, Foretz M, Scorrano L, Rudolf R, Sandri M (2010) Mitochondrial fission and remodelling contributes to muscle atrophy. *EMBO J.* **29**, 1774–1785.

Saks VA, Veksler VI, Kuznetsov AV, Kay L, Sikk P, Tiivel T, Tranqui L, Olivares J, Winkler K, Wiedemann F, Kunz WS (1998) Permeabilized cell and skinned fiber techniques in studies of mitochondrial function in vivo. *Mol. Cell. Biochem.* **184**, 81–100.

Saks V, Guzun R, Timohhina N, Tepp K, Varikmaa M, Monge C, Beraud N, Kaambre T, Kuznetsov A, Kadaja L, Eimre M, Seppet E (2010) Structure-function relationships in feedback regulation of energy fluxes in vivo in health and disease: mitochondrial interactosome. *Biochim. Biophys. Acta* **1797**, 678–697.

Schafer E, Seelert H, Reifschneider NH, Krause F, Dencher NA, Vonck J (2006) Architecture of active mammalian respiratory chain supercomplexes. *J. Biol. Chem.* **281**, 15370–15375.

Schwerzmann K, Hoppeler H, Kayar SR, Weibel ER (1989) Oxidative capacity of muscle and mitochondria: correlation of physiological, biochemical, and morphometric characteristics. *Proc. Natl. Acad. Sci. U.S.A.* **86**, 1583–1587.

Seo AY, Xu J, Servais S, Hofer T, Marzetti E, Wohlgemuth SE, Knutson MD, Chung HY, Leeuwenburgh C (2008) Mitochondrial iron accumulation with age and functional consequences. *Aging Cell* **7**, 706–716.

Shaw CS, Jones DA, Wagenmakers AJ (2008) Network distribution of mitochondria and lipid droplets in human muscle fibres. *Histochem. Cell Biol.* **129**, 65–72.

Short KR, Bigelow ML, Kahl J, Singh R, Coenen-Schimke J, Raghavakaimal S, Nair KS (2005) Decline in skeletal muscle mitochondrial function with aging in humans. *Proc. Natl. Acad. Sci. U.S.A.* **102**, 5618–5623.

Siu PM (2009) Muscle apoptotic response to denervation, disuse, and aging. *Med. Sci. Sports Exerc.* **41**, 1876–1886.

Siu PM, Pistilli EE, Butler DC, Alway SE (2005) Aging influences cellular and molecular responses of apoptosis to skeletal muscle unloading. *Am. J. Physiol. Cell Physiol.* **288**, C338–C349.

Stowe DF, Camara AK (2009) Mitochondrial reactive oxygen species production in excitable cells: modulators of mitochondrial and cell function. *Antioxid. Redox Signal.* **11**, 1373–1414.

St-Pierre J, Drori S, Uldry M, Silvaggi JM, Rhee J, Jager S, Handschin C, Zheng K, Lin J, Yang W, Simon DK, Bachoo R, Spiegelman BM (2006) Suppression of reactive oxygen species and neurodegeneration by the PGC-1 transcriptional coactivators. *Cell* **127**, 397–408.

Strasser H, Tiefenthaler M, Steinlechner M, Eder I, Bartsch G, Konwalinka G (2000) Age dependent apoptosis and loss of rhabdosphincter cells. *J. Urol.* **164**, 1781–1785.

Terman A, Brunk UT (2004) Myocyte aging and mitochondrial turnover. *Exp. Gerontol.* **39**, 701–705.

Thomas MM, Khan W, Betik AC, Wright KJ, Hepple RT (2010) Initiating exercise training in late middle age minimally protects muscle contractile function and increases myocyte oxidative damage in senescent rats. *Exp. Gerontol.* in press, DOI 20643203.

Tonkonogi M, Fernstrom M, Walsh B, Ji LL, Rooyackers O, Hammarqvist F, Wernerman J, Sahlin K (2003) Reduced oxidative power but unchanged antioxidative capacity in skeletal muscle from aged humans. *Pflugers Arch.* **446**, 261–269.

Treberg JR, Quinlan CL, Brand MD (2010) Hydrogen peroxide efflux from muscle mitochondria underestimates matrix superoxide production – a correction using glutathione depletion. *FEBS J.* **277**, 2766–2778.

Trounce I, Byrne E, Marzuki S (1989) Decline in skeletal muscle mitochondrial respiratory chain function: possible factor in ageing. *Lancet* **1**, 637–639.

Vasilaki A, Mansouri A, Remmen H, van der Meulen JH, Larkin L, Richardson AG, McArdle A, Faulkner JA, Jackson MJ (2006) Free radical generation by skeletal muscle of adult and old mice: effect of contractile activity. *Aging Cell* **5**, 109–117.

Vonck J, Schafer E (2009) Supramolecular organization of protein complexes in the mitochondrial inner membrane. *Biochim. Biophys. Acta* **1793**, 117–124.

Wanagat J, Cao Z, Pathare P, Aiken JM (2001) Mitochondrial DNA deletion mutations colocalize with segmental electron transport system abnormalities, muscle fiber atrophy, fiber splitting, and oxidative damage in sarcopenia. *FASEB J.* **15**, 322–332.

Wenz T, Rossi SG, Rotundo RL, Spiegelman BM, Moraes CT (2009) Increased muscle PGC-1alpha expression protects from sarcopenia and metabolic disease during aging. *Proc. Natl. Acad. Sci. U.S.A.* **106**, 20405–20410.

Zoratti M, Szabo I (1995) The mitochondrial permeability transition. *Biochim. Biophys. Acta* **1241**, 139–176.

Supporting Information

Additional supporting information may be found in the online version of this article:

Fig. S1 Confocal imaging shows lower mitochondrial content in SEN isolated mitochondrial preparations.

Fig. S2 Representative traces of mitochondrial respiration.

As a service to our authors and readers, this journal provides supporting information supplied by the authors. Such materials are peer-reviewed and may be re-organized for online delivery, but are not copy-edited or typeset. Technical support issues arising from supporting information (other than missing files) should be addressed to the authors.